Steel and Composite Structures, Vol. 5, No. 1 (2005) 1-15
DOI: http://dx.doi.org/10.12989/scs.2005.5.1.001

Buckling of sandwich cylindrical shells under axial loading

Mitao Ohga† and Aruna Sanjeewa Wijenayaka‡

Department of Civil and Environmental Engineering, Ehime University, 3, Bunkyo-Cho, Matsuyama 790-8577, Japan

James G. A. Croll‡†

Department of Civil and Environmental Engineering, University Collage of London, London WC1E 6BT, U.K.

(Received January 27, 2004, Accepted January 24, 2005)

Abstract. Important characteristics of the previously proposed reduced stiffness method and a summery of its design curves for the buckling of the axially loaded sandwich cylindrical shells is presented. Comparison of the lower bound obtained with FEM analysis with that from the reduced stiffness analysis shows that the proposed reduced stiffness method can provide safe lower bounds for the buckling of geometrically imperfect, axially loaded sandwich cylindrical shells. One of the attractive features of the reduced stiffness elastic lower bound analysis is that it provides safe estimates of buckling loads that do not depend on the specification of the precise magnitude of the imperfection spectra. As a result, designers can readily apply this method without being worried about possible geometrical imperfections that might be generated during fabrication and construction of sandwich cylindrical shells.

Key words: sandwich shells; reduced stiffness; buckling; lower bound; axial loading.

1. Introduction

The light-core sandwich construction has been identified as an alternative to conventional thin walled structures due to its higher stiffness/weight and strength/weight ratios. As a result, sandwich construction results in lower lateral deformation, higher buckling resistance, and higher natural frequencies than do other single-material constructions. Such advantages will insure that the sandwich construction will continue to be in demand (Vinson 1999). Among many types of sandwich constructions, the sandwich cylindrical shell is continuing to find many applications as an axially compressed structure in civil, mechanical, offshore, and aerospace engineering. Its ever expanding applications have created many imperfectly understood problems such as imperfection sensitivity, shear instability and buckling.

†Professor, Corresponding author, E-mail: ohga@dpc.ehime-u.ac.jp
‡Ph.D Student
‡†Professor

Cylinders are unfavorably sensitive to initial geometric imperfections such that they can collapse under a fraction of the strength of the perfect shell (Nemeth and Starnes 1998). Recently, it has been realized that the initial imperfection in the sandwich cylindrical shell structure combined with the highly unstable forms of post buckling behavior is responsible for the scatter of the buckling loads below that of predicted by the classical buckling analysis (Croll 1981, 1995, Ohga and Umakoshi 2001). In this regard, a reduced stiffness analysis method would not only provide a safe lower bound, but also simplify the design of the sandwich cylindrical shell. Therefore, a Reduced Stiffness (RS) method has been proposed for the estimation of the lower bound of the buckling of the sandwich cylindrical shell (Ohga and Umakoshi 2001).

In this paper, important characteristic of the proposed reduced stiffness method are discussed. In addition, the reduced stiffness design curves for the axially loaded sandwich cylindrical shell are summarized. This process begins with classical buckling analysis of the shell and identifying those energy components that adversely affect the stability of the shell. Elimination of so identified energy components from the total potential energy leads to the derivation of the reduced stiffness lower bound. The accuracy of the proposed reduced stiffness lower bound is verified by comparing it with that obtained with FEM analysis of the geometrically imperfect sandwich cylindrical shell. This FEM program employs so-called 9-node isoparametric shell element with three displacement and two rotational displacement degrees of freedom at each nodal point for discretization of the model. The use of the isoparametric shell element allows layered analysis of the sandwich cylindrical shell and, as a result, allows different material properties through the thickness of the cylinder.

One of the attractive features of the proposed elastic lower bound analysis is that it provides safe estimates of buckling loads that do not depend on the specification of the precise magnitude of the imperfection spectra. Therefore, designers can readily apply this method to design sandwich cylindrical shell without being worried about potential geometric imperfections that might be generated as a result of mishandling during fabrication, eruption, earthquakes etc.

2. RS buckling strength of the axially loaded sandwich cylindrical shell

2.1. Total potential energy of an axially loaded sandwich cylindrical shell

In the classical analysis of a sandwich cylinder of length L, mean radius a, face thickness h_f and core thickness h_c (Fig. 1), a convenient way of examining the various possible equilibrium paths described by the stationarity of the total potential energy is to first define the membrane fundamental state. Assuming that the axial load is supported only by the inner and outer faces while the core supports only transverse shear (Fig. 2), the fundamental state of the present problem can be given as

$$(N_x^F, N_s^F, N_{xs}^F) = (-2\sigma h_f, 0, 0) \tag{1a}$$

$$(M_x^F, M_s^F, M_{xs}^F) = (0, 0, 0) \tag{1b}$$

Here, N_x^F, N_s^F and N_{xs}^F are the membrane fundamental stresses and M_x^F, M_s^F and N_{xs}^F denotes relevant moments. Corresponding strains E_x^F, E_s^F and E_{xs}^F can be written as

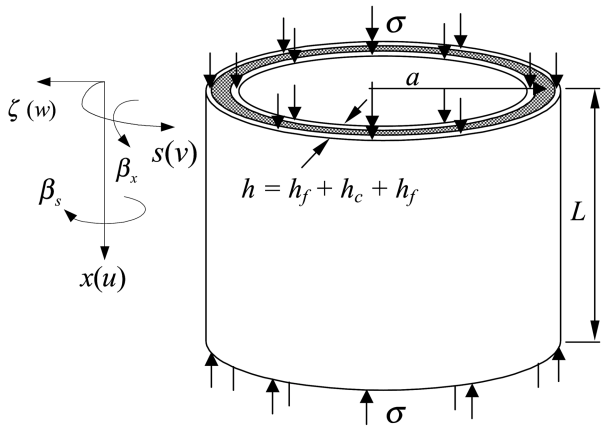

Fig. 1 Geometry, axis system, and the applied loads of the axially loaded sandwich cylindrical shell

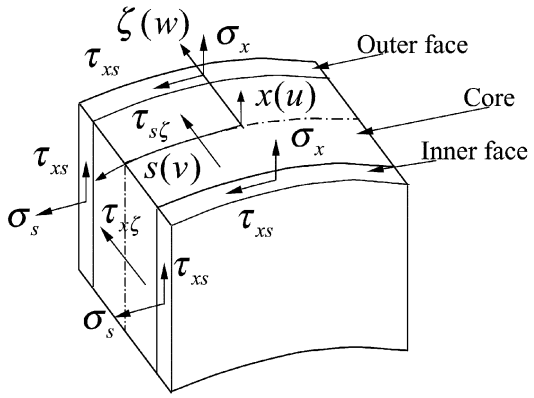

Fig. 2 Element of a sandwich shell, stresses in the core and faces

$$(E_x^F, E_s^F, E_{xs}^F) = (-\sigma/E_f, \nu_f\sigma/E_f, 0) \tag{2}$$

Where, σ is the externally applied axial stress, E_f; the modulus of elasticity of face material and ν_f; the Poisson's ratio of the face material.

At the bifurcation from the fundamental state, depending on the incremental membrane strains that are linear (ε_x', ε_s', ε_{xs}') and quadratic (ε_x'', ε_s'', ε_{xs}''), the constant, linear, quadratic components of the total potential energy can be written as

$$\Pi = \Pi_0 + \Pi_1 + \Pi_2 + \Pi_3 + \ldots\ldots \tag{3}$$

$$\Pi_0 = \frac{1}{2}\iiint (N_x^F E_x^F + N_s^F E_s^F) ds dx d\zeta - \iiint \sigma U^F ds dx d\zeta \tag{4a}$$

$$\Pi_1 = \frac{1}{2}\iiint [(N_x^F \varepsilon_x' + \sigma_x' E_x^F) + (N_s^F \varepsilon_s' + \sigma_s' E_s^F)] ds dx d\zeta - \iint \sigma u ds d\zeta \tag{4b}$$

$$\Pi_2 = \frac{1}{2}\iiint [\sigma_x' \varepsilon_x' + \sigma_s' \varepsilon_s' + \tau_{xs}' \gamma_{xs}' + \tau_{x\zeta}' \gamma_{x\zeta}' + \tau_{s\zeta}' \gamma_{s\zeta}'] ds dx d\zeta$$

$$+\frac{1}{2}\int\int(N_x^F\varepsilon_x'' + \sigma_x''E_x^F)dsdx + \frac{1}{2}\int\int(\sigma_s''E_s^F)dsdx = U + V^x + V^s \tag{4c}$$

Where, U is the sum of strain energies. While, V^x and V^s denote the non-linear membrane energy components in axial and circumferential direction respectively. By employing the sine convention and the notations given in Fig. 2, the linear incremental membrane stress resultants σ_x', σ_s', τ_{xs}', $\tau_{x\zeta}'$, and $\tau_{s\zeta}'$ in Eq. (4) can be given as

$$\sigma_x' = D_f(\varepsilon_x' + \nu_f\,\varepsilon_s') \tag{5a}$$

$$\sigma_s' = D_f(\varepsilon_s' + \nu_f\,\varepsilon_x') \tag{5b}$$

$$\tau_{xs}' = G_f\,\gamma_{xs}' \tag{5c}$$

$$\tau_{x\zeta}' = G_c\,\gamma_{x\zeta}' \tag{5d}$$

$$\tau_{s\zeta}' = G_c\,\gamma_{s\zeta}' \tag{5e}$$

Here, G_c and G_f denote the core and face material shear strengths respectively. Further, $D_f = E_f/(1-\nu_f^2)$. The linear incremental stresses (Eq. (5)) associate with the linear strains defined by the orthogonal curvilinear coordinate system (x, s, ζ) given in Fig. 1. They can be given as

$$\varepsilon_x' = \frac{\partial u}{\partial x} + \zeta\frac{\partial\beta_x}{\partial x} = \varepsilon_{x0} + \zeta k_x \tag{6a}$$

$$\varepsilon_s' = \frac{\partial v}{\partial s} + \frac{w}{a} + \zeta\frac{\partial\beta_s}{\partial s} = \varepsilon_{s0} + \zeta k_s \tag{6b}$$

$$\gamma_{xs}' = \frac{\partial v}{\partial x} + \frac{\partial u}{\partial s} + \zeta\left(\frac{\partial\beta_s}{\partial x} + \frac{\partial\beta_x}{\partial s}\right) = \gamma_{xs0} + \zeta k_{xs} \tag{6c}$$

$$\gamma_{x\zeta}' = \frac{\partial w}{\partial s} + \beta_x \tag{6d}$$

$$\gamma_{s\zeta}' = \frac{\partial w}{\partial s} - \frac{v}{a} + \beta_s \tag{6e}$$

The non-linear stresses σ_x'', and σ_s'' in Eq. (4c) that results from the fundamental state Poisson expansion can be given as

$$\sigma_x'' = D_f(\varepsilon_x'' + \nu_f\,\varepsilon_s'') \tag{7a}$$

$$\sigma_s'' = D_f(\varepsilon_s'' + \nu_f\,\varepsilon_x'') \tag{7b}$$

They associate with the non-linear strain components,

$$\varepsilon_x'' = \frac{1}{2}\left(\frac{\partial w}{\partial x}\right)^2 = \frac{1}{2}(w_x')^2 \tag{8a}$$

$$\varepsilon_s'' = \frac{1}{2}\left(\frac{\partial w}{\partial x}\right)^2 = \frac{1}{2}(w_s')^2 \tag{8b}$$

2.2. Displacement functions

Assuming that the cylindrical sandwich shell is simply supported at the ends, the displacements (u, v, w) in the directions of (x, s, ζ) and rotations (β_x, β_s) about the s and x axes (Fig. 1) can be formulated into displacement functions.

$$u = A_1 \cos \alpha s \cos \rho x \tag{9a}$$

$$v = A_2 \sin \alpha s \sin \rho x \tag{9b}$$

$$w = A_3 \cos \alpha s \sin \rho x \tag{9c}$$

$$\beta_x = A_4 \cos \alpha s \cos \rho x \tag{9d}$$

$$\beta_s = A_5 \sin \alpha s \sin \rho x \tag{9e}$$

In which, $\alpha = n/a$, $\rho = m\pi/L$. Here m denotes the axial half-wave number and n, the circumferential full-wave number. A_i is the amplitude of the displacement function.

2.3. Classical buckling strength

Of the present concern is the quadratic component Π_2 of the total potential energy for it is that controls the critical behavior and from which the homogeneous equations yielding the critically stable state is derived. From Eq. (4c), first variation of the quadratic component Π_2 can be written as

$$\begin{aligned}\delta\Pi_2 = {} & \iiint [\sigma_x' \delta\varepsilon_x' + \sigma_s' \delta\varepsilon_s' + \tau_{xs}' \delta\gamma_{xs}' + \tau_{x\zeta}' \delta\gamma_{x\zeta}' + \tau_{s\zeta}' \delta\gamma_{s\zeta}'] ds dx d\zeta \\ & + \iint \{(N_x^F \delta\varepsilon_x'') + D_f(\delta\varepsilon_x'' + \nu_f \delta\varepsilon_s'') E_x^F\} ds dx \\ & + \iint D_f(\delta\varepsilon_s'' + \nu_f \delta\varepsilon_x'') E_s^F ds dx = \delta U + \delta V^x + \delta V^s \end{aligned} \tag{10}$$

Application of the variational principles to Eq. (10) in the presence of the stress-strain relations from Eqs. (5) and (7), strain-displacement relations from Eqs. (6) and (8) and displacement functions from Eq. (9) result in a set of homogeneous equations;

$$\begin{bmatrix} c_{11} & c_{12} & c_{13} & & c_{14} & c_{15} \\ c_{21} & c_{22} & c_{23} & & c_{24} & c_{25} \\ c_{31} & c_{32} & c_{33} & -\lambda\sigma & c_{34} & c_{35} \\ c_{41} & c_{42} & c_{43} & & c_{44} & c_{45} \\ c_{51} & c_{52} & c_{53} & & c_{54} & c_{55} \end{bmatrix} \begin{bmatrix} A_1 \\ A_2 \\ A_3 \\ A_4 \\ A_5 \end{bmatrix} = 0 \tag{11}$$

Where the coefficients (C_{ij}=C_{ji}) are obtained as

$$C_{11} = \rho^2 D_{M1} + \alpha^2 D_{M2};\ C_{12} = -(\nu_f \alpha\rho D_{M1} + \alpha\rho D_{M2});\ C_{13} = -\frac{\nu_f}{a}\rho D_{M1};\ C_{14} = C_{15} = 0$$

$$C_{21} = \alpha^2 D_{M1} + \rho^2 D_{M2} + \frac{S_s}{a^2};\ C_{23} = \frac{\alpha}{a} D_{M1} + \frac{\alpha}{a} S_s;\ C_{24} = 0;\ C_{25} = -\frac{S_s}{a}$$

$$C_{33} = \frac{1}{a^2}D_{M1} + \rho^2 S_x + \alpha^2 S_s;\ C_{34} = \rho S_x;\ C_{35} = -\alpha S_s;\ C_{44} = \rho^2 D_{B1} + \alpha^2 D_{B2} + S_x$$

$$C_{45} = -(\nu_f\ \alpha\rho D_{B1} + \alpha\rho D_{B2});\ C_{55} = \alpha^2 D_{B1} + \rho^2 D_{B2} + S_s$$

$$\lambda = \rho^2\left\{h_f + \frac{D_{M1}}{2E_f}(1-\nu_f)\right\}$$

Where, the membrane, bending and shear stiffness are obtained as

$$D_{M1} = \frac{2E_f}{(1-\nu_f)}h_f\ ;\ D_{M2} = 2h_f G_f;\ D_{B1} = \frac{E_f}{12(1-\nu_f^2)}\{(h_c + 2h_f)^3 - h_c^3\}$$

$$D_{B2} = \frac{G_f}{12}\{(h_c + 2h_f)^3 - h_c^3\};\ S_x = G_c h_c;\ S_s = G_c h_c$$

By solving Eq. (11), amplitudes A_1, A_2, A_4, and A_5 of the displacement functions can be obtained as a function of A_3.

$$A_1 = \frac{C_{12}A_2' + C_{13}}{C_{11}}A_3 = A_1' A_3 \tag{12a}$$

$$A_2 = \frac{(C_{12}C_{13} - C_{11}C_{23})(C_{45}^2 - C_{44}C_{55}) + (C_{11}C_{25})(C_{34}C_{45} - C_{35}C_{44})}{C_{11}C_{25}^2 C_{44} - (C_{12}^2 - C_{11}C_{22})(C_{45}^2 - C_{44}C_{55})}A_3 = A_2' A_3 \tag{12b}$$

$$A_4 = -\frac{(C_{34} + C_{45}A_5')}{C_{44}}A_3 = A_4' A_3 \tag{12c}$$

$$A_5 = \frac{(C_{12}C_{13} - C_{11}C_{23})(-C_{25}C_{44}) - (C_{34}C_{45} - C_{35}C_{44})(C_{12}^2 - C_{11}C_{22})}{(C_{12}^2 - C_{11}C_{22})(C_{45}^2 - C_{44}C_{55}) - C_{11}C_{25}^2 C_{44}}A_3 = A_5' A_3 \tag{12d}$$

The classical axial buckling strength is obtained as

$$\sigma_c = \frac{1}{\lambda}(C_{31}A_1' + C_{32}A_2' + C_{33} + C_{34}A_4' + C_{35}A_5') \tag{13}$$

The critical axial and circumferential mode numbers and relevant classical buckling strength are obtained by the numerical iteration of Eq. (13). By applying $\sigma_c = q_c/2h_f$ in the above equation, classical critical buckling load per unit run on the circumference of the sandwich shell is obtained as

$$q_c = \frac{2h_f}{\lambda}(C_{31}A_1' + C_{32}A_2' + C_{33} + C_{34}A_4' + C_{35}A_5') \tag{14}$$

$$k_c = \frac{q_c}{2E_f\ h_f} \tag{15}$$

Here, k_c denotes the classical critical buckling coefficient.

2.4. Reduced stiffness buckling strength

In the lower bound buckling analysis, the membrane, bending and shear energies of quadratic component of the total potential energy are well analyzed for their behaviors during the buckling process. In this way, those energy components that contribute to the stabilization of the axially loaded sandwich cylindrical shell are identified. In addition, those that are at risk through the combined action of mode interaction and imperfections are identified. Loss of such energy components has destructive effects on the sandwich cylindrical shell's axial load carrying capacity and, therefore, can adversely affect the stability of the shell. Therefore, these energy components are eliminated to derive the reduced stiffness model (Croll 1981, Ohga and Wijenayaka 2003).

From Eq. (4c), quadratic component Π_2 can be written as

$$\Pi_2 = U_M + U_B + U_S + V_M^x + V_M^s \tag{16}$$

Where, U_M, U_B and U_S are the membrane, bending and shear energies respectively. Their components in relevant directions and planes can be written as

$$U_M = U_M^x + U_M^s + U_M^{sx} \tag{17a}$$

$$U_B = U_B^x + U_B^s + U_B^{sx} \tag{17b}$$

$$U_S = U_S^{x\zeta} + U_S^{s\zeta} \tag{17c}$$

The energy components in Eq. (17) can be given as

$$U_M^x = \frac{1}{2}\iint\{D_{M1}(\varepsilon_{x0} + \nu_f \varepsilon_{s0})\varepsilon_{x0}\}dsdx \tag{18a}$$

$$U_M^s = \frac{1}{2}\iint\{D_{M1}(\varepsilon_{s0} + \nu_f \varepsilon_{x0})\varepsilon_{s0}\}dsdx \tag{18b}$$

$$U_M^{xs} = \frac{1}{2}\iint\{D_{M1}\gamma_{xs0}\gamma_{xs0}\}dsdx \tag{18c}$$

$$U_B^x = \frac{1}{2}\iint\{D_{B1}(k_x + \nu_f k_s)k_x\}dsdx \tag{18d}$$

$$U_B^s = \frac{1}{2}\iint\{D_{B1}(k_s + \nu_f k_x)k_s\}dsdx \tag{18e}$$

$$U_B^{xs} = \frac{1}{2}\iint\{D_{B2}k_{xs0}k_{xs0}\}dsdx \tag{18f}$$

$$U_S^{x\zeta} = \frac{1}{2}\iint\{S_x\gamma_{x\zeta}\gamma_{x\zeta}\}dsdx \tag{18g}$$

$$U_S^{s\zeta} = \frac{1}{2}\iint\{S_s\gamma_{s\zeta}\gamma_{s\zeta}\}dsdx \tag{18h}$$

V_M^x and V_M^s are the contributions arising from the non-linear stresses and strains, as given in Eq. (19a) and Eq. (19b) below,

$$V_M^x = \frac{1}{2}\iint (N_x^F \varepsilon_x'' + \sigma_x'' E_x^F) ds dx$$

$$= -q\frac{1}{2}\iint \left\{ \frac{1}{2}(w_x')^2 + \frac{1}{4h_f E_f} D_{M1}((w_x')^2 + \nu_f (w_s')^2) \right\} ds dx = q\bar{V}_M^x \tag{19a}$$

$$V_M^s = \frac{1}{2}\iint (\sigma_s'' E_s^F) ds dx$$

$$= q\frac{1}{2}\iint \left\{ \frac{\nu_f}{4h_f E_f} D_{M1}((w_s')^2 + \nu_f (w_x')^2) \right\} ds dx = q\bar{V}_M^s \tag{19b}$$

By substituting Eq. (19) in Eq. (16) and considering the stationary condition of the quadratic component Π_2 of the potential energy, the classical critical buckling strength q_c can be written as

$$U_M + U_B + U_S + q_c(\bar{V}_M^s + \bar{V}_M^x) = 0 \tag{20}$$

In Eq. (19b), the circumferential contribution V_M^s arises entirely from the fundamental circumferential strain E_s^F that results from the Poisson expansion when the cylindrical sandwich shell is axially loaded. Furthermore, and it is for this reason that this circumferential term is of such significance, that it depends on non-linear hoop stress σ_s'' and it is positive definite regardless of the form of the critical deformation, i.e., the non-linear circumferential energy together with the strain energy components will contribute to the stabilization in the critical mode. Virtually, all the destabilization arises form the non-linear axial term V_M^x.

Mode coupling can result the non-linear circumferential membrane energy, V_M^s being counter balanced by the linear axial membrane energy, U_M^x (Croll and Batista 1981, Ohga and Wijenayaka 2003). As a result, the stabilization provided by both the energy components is lost. Therefore, elimination of these two energy components leads to the reduced incremental quadratic potential energy. The reduced stiffness buckling strength (q_{rs}) is derived from the reduced incremental quadratic potential energy.

$$U_M^s + U_M^{xs} + U_B + U_S + q_{rs}(\bar{V}_M^x) = 0 \tag{21}$$

From Eqs. (20) and (21), the reduced stiffness buckling strength can be obtained as a function of classical buckling strength.

$$q_{rs} = q_c \left(\frac{U_M^s + U_M^{xs} + U_B + U_S}{U_M + U_B + U_S} \right) \left(\frac{\bar{V}_M^x + \bar{V}_M^s}{\bar{V}_M^x} \right) \tag{22}$$

The critical axial and circumferential mode numbers and relevant reduced stiffness buckling strength are obtained by the numerical iteration of Eq. (22). Similarly, the reduced stiffness buckling coefficient can be obtained as a function of classical buckling coefficient.

$$k_{rs} = k_c \left(\frac{U_M^s + U_M^{xs} + U_B + U_S}{U_M + U_B + U_S} \right) \left(\frac{\bar{V}_M^x + \bar{V}_M^s}{\bar{V}_M^x} \right) \tag{23}$$

3. Characteristic of reduced stiffness buckling strength

The minimum reduced stiffness buckling coefficient (k_{rs}) [Eq. (23)] occurs when the axial half-wave number is minimum as can be seen in Fig. 3. It reaches the unique minimum at a particular circumferential wave number. The critical stress corresponding to this reduced stiffness critical mode can be expected to provide the least possible resistance of the shell to incremental displacements in the post-critical region (Croll and Batista 1981). However, the classical buckling coefficient (k_c) [Eq. (15)] is almost constant irrespective of the circumferential wave number.

Variation of the classical buckling coefficient (k_c) [Eq. (15)] and the RS buckling coefficient (k_{rs}) [Eq. (23)] with the parameter L/a are given in Fig. 4. Here, $V(=E_f h_f / 4aG_c(1-\nu_f^2))$ is the transverse shear flexibility parameter. As can be seen in this figure, the reduced stiffness buckling coefficient reduces as the length of the cylinder increases. On the other hand, the classical buckling coefficient is almost constant with L/a. The classical critical buckling mode shape consists of number of axial half-waves and that increases as L/a increases. This helps to maintain the classical buckling coefficient at a constant value even when L/a increases. However, the critical reduced stiffness mode shape consists of only one axial half-wave. As a result, the reduced stiffness buckling coefficient reduces as L/a increases. Further, all three curves of reduced stiffness buckling coefficient merge to one line as the L/a increases. This implies that the critical RS buckling coefficient becomes independent of the core material shear strength as L/a increases. Or in other words, the contribution of the core to the buckling strength of the shell becomes comparatively less. Further, both classical and RS buckling coefficients corresponding to V=0.01 and V=0.0 are almost equal. This characteristic is discussed below.

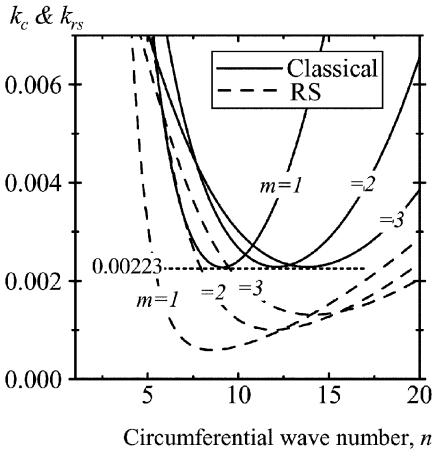

Fig. 3 Classical and RS spectra (L/a=1.0, V=0.01, E_f=2.05×10^5 MPa, ν_f= 0.3, a/h_f= 5000, h_c/h_f=10, a =1.0 m)

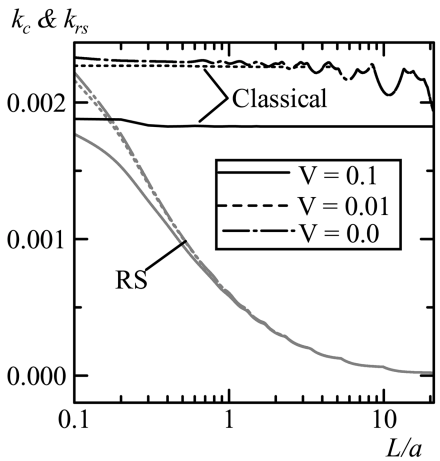

Fig. 4 Variation of classical and RS buckling coefficients with L/a (E_f=2.05×10^5 MPa, ν_f=0.3, a/h_f=5000, h_c/h_f=10, a=1.0 m)

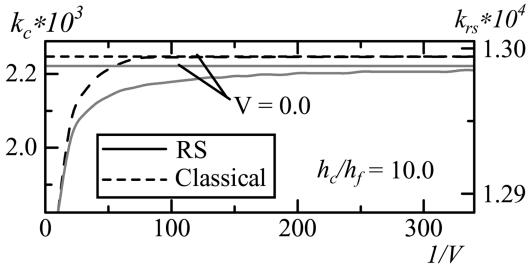

Fig. 5 Variation of classical and RS buckling coefficients with $1/V$ (E_f=2.05×10^5 MPa, v_f=0.3, L/a =5.0, a/h_f=5000, a=1.0 m)

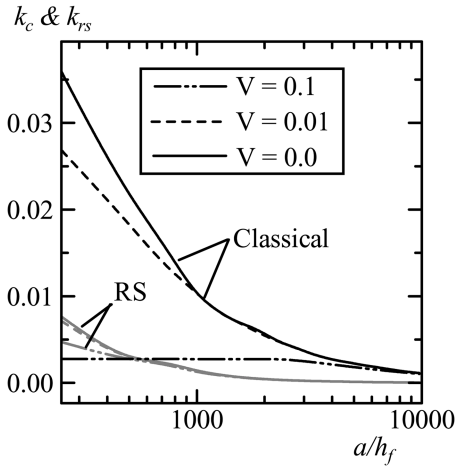

Fig. 6 Variation of classical and RS buckling coefficients with a/h_f (L/a=5.0, E_f=2.05×10^5 MPa, v_f=0.3, a/h_f=5000, h_c/h_f=10, a=1.0 m)

Variation of k_c [Eq. (15)], and k_{rs} [Eq. (23)] with $1/V$ is given in Fig. 5 (L/a=5.0). Both seem to have a similar behavior with $1/V$. And, the critical classical and RS buckling coefficients asymptotically reach the value corresponding to V equals zero (G_c= ∞). When $1/V$>200, the rate of increase of both k_c and k_{rs} are almost zero. This implies that the gain in the buckling strength by a certain increment of the core shear strength when $1/V$ >200 is comparatively less compared to the gain by the same increment when $1/V$ <200. Thus, the reduced stiffness buckling strength of the axially loaded sandwich cylindrical shell is hardly improved by increasing the core shear strength at its higher values. The very same was observed even when L/a increased.

The variation of k_c [Eq. (15)], and k_{rs} [Eq. (23)] with a/h_f are examined in Fig. 6 (L/a=5.0). As it is evident in this figure both reduced stiffness and classical buckling coefficients have similar variations that all three cases of V in both the classical and RS method merge as the ratio a/h_f increases. This implies that as the ratio a/h_f increases the contribution from the core material shear strength to the buckling strength reduces. The reduced stiffness buckling coefficient curves seem to merge faster than that of classical buckling coefficient.

4. Geometrically nonlinear analysis of the sandwich cylindrical shell

A nonlinear analysis method has been developed into a finite-element code to allow investigation of the behavior of geometrically imperfect sandwich cylindrical shells. The validity of the proposed method is assessed by comparing the reduced stiffness lower bound with that obtained with FEM analysis of geometrically nonlinear sandwich cylindrical shells.

The FEM program developed for this purpose employs so called 9-node isoparametric shell element for the discretization of the model. Five degrees of freedom are specified at each nodal point corresponding to its three displacements and two rotations. The use of the isoparametric shell element allows layered analysis and, as a result, different material properties through the thickness of the sandwich cylindrical shell.

5. FEM lower bound buckling analysis

FEM buckling analysis of sandwich cylindrical shells having L/a=0.5, 1.0 2.0, 3.0, 5.0, 7.0 and 10.0 were selected for numerical examples. In addition, each model was considered for $V(=E_f h_f / 4aG_c(1-\nu_f^2))$ equals 0.1, 0.01, and 0.0 ($G_c = \infty$). V equals 0.1 corresponds to a very weak core and represents the normal cross section. The critical mode shape from the reduced stiffness method was introduced as the initial geometric imperfection in the FEM analysis as it is expected to provide the least resistance in the post-critical region. The analyses were carried out by magnifying the amplitude of the initial deformation (w_0/h), where, w_0 is the initial lateral deformation while h is the total thickness of the cylinder. The stress resultant from FEM analysis was taken as σ_{fem}. The resulting equilibrium path curves for L/a=1.0 (V=0.1, 0.01, 0.0) are given in Figs. 7(a), (b) and (c) respectively. These equilibrium path curves were obtained by plotting the stress parameter (σ_{fem}/σ_c) with the respective lateral deformation (w/h). As it can be seen in those figures, the variation of a typical curve is such that the stress peaks up at a certain point and then reduces as the deformation develops. Moreover, the maximum stress parameter ($\sigma_{fem}^{\max}/\sigma_c$) of the equilibrium path seems to decrease as the magnitude of the initial imperfection increases. The curve corresponding to w_0/h equals 2.5 is special that beyond this curve the above mentioned peaking does not appear. This curve is named as the 'limiting equilibrium path' and the maximum stress parameter on the same ($\sigma_{fem}^{low}/\sigma_c$) is taken as the lower bound from the FEM analysis. The post-buckling deformation shapes corresponding to all three cases of transverse shear flexibility parameters (V=0.1, 0.01, 0.0) are similar to each other and the one corresponding to V=0.01 and w_0/h=1.5 is shown in Fig. 7(d). All selected numerical examples gave similar results to that of Figs. 7(a), (b) and (c). Further, the classical and Plantema(1966) buckling strengths are given in Fig. 7. Both the methods give almost equal results. However, the reduced stiffness and FEM lower bounds occur well below the results obtained from classical and Plantema methods.

When the maximum stress parameter ($\sigma_{fem}^{\max}/\sigma_c$) on each equilibrium path shown with 'dot marks' in Fig. 7 is plotted against the respective initial imperfection, that results in the imperfection sensitivity plot. The same for particular example of L/a=1.0 and 3.0 are given in Figs. 8(a) and (b) respectively. As it can be seen in these figures, each curve of V=0.1, 0.01, and 0.0 asymptotically reach from and above the relevant reduced stiffness buckling strengths. Moreover, the above-mentioned FEM lower bound ($\sigma_{fem}^{low}/\sigma_c$) appears above that from reduced stiffness analysis. As a result, it is evident that the proposed reduced stiffness method provides safe lower bounds for axially loaded sandwich cylindrical shell for all possible transverse shear flexibility parameters (V). In other words, the reduced stiffness method provides safe lower bounds for all possible core shear strengths.

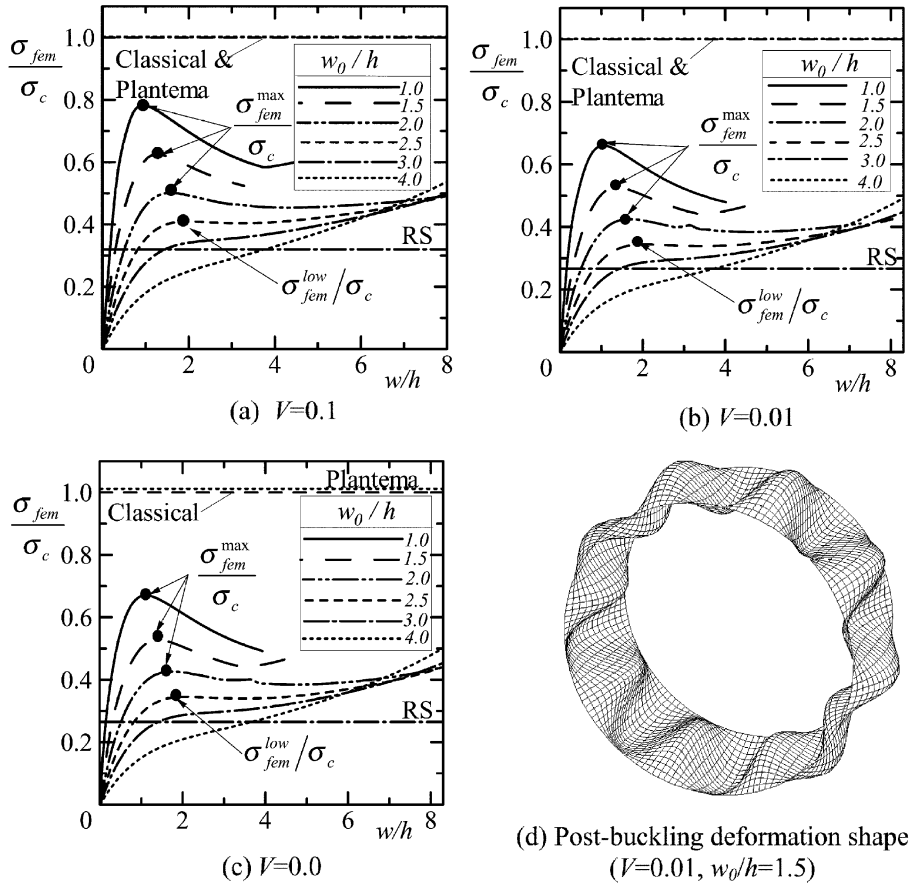

Fig. 7 FEM buckling analysis of geometrically imperfect sandwich cylinder (L/a=1.0, V=0.01, E_f =2.05×10^5 MPa, ν_f=0.3, a/h_f=5000, h_c/h_f=10, a=1.0 m)

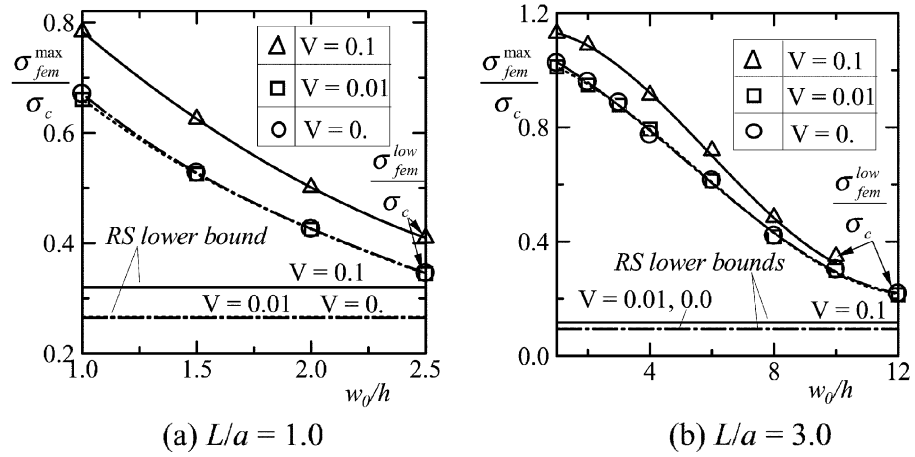

Fig. 8 Imperfection sensitivity of the sandwich shells (E_f=2.05×10^5 MPa, ν_f=0.3, a/h_f=5000, h_c/h_f=10, a=1.0 m)

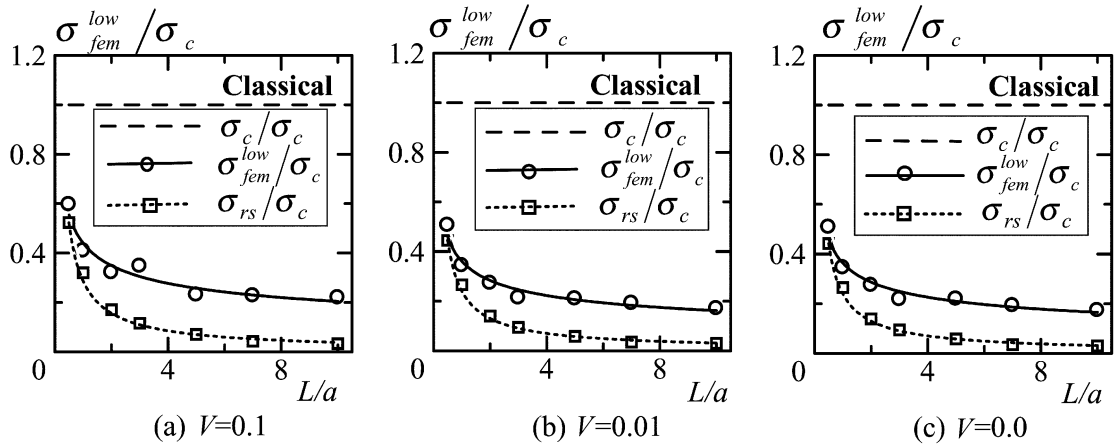

Fig. 9 Variation of the FEM and reduced stiffness lower bounds with L/a (E_f =2.05×10^5 MPa, ν_f=0.3, a/h_f=5000, h_c/h_f=10, a=1.0 m)

Figs. 9 (a), (b) and (c) show the variation of the reduced stiffness strengths (σ_{rs}/σ_c) and FEM lower bound ($\sigma_{fem}^{low}/\sigma_c$) with L/a for shells having V=0.1, 0.01 and 0.0. Both show a similar trend of variation as L/a increases; there is a sharp descend when L/a<5. However, this descend is comparatively small when L/a>5. In addition, as it can be seen in Fig. 9, the reduced stiffness lower bound is obtained bellow that from the FEM analysis for all core shear strengths. This implies that the proposed reduced stiffness method provides explicit and safe lower bounds for the axially loaded sandwich cylindrical shell.

6. Conclusions

Conclusive remarks of the classical and reduced stiffness methods are summarized here. These conclusions are based on their characteristics and can be considered in the design process.

1. Different reduced stiffness buckling coefficient curves corresponding to different shear strengths of core merge to one line as L/a increases. This implies that as L/a increases, the reduced stiffness buckling strength becomes independent of the core material shear strength. In addition, the reduced stiffness buckling coefficient gradually decrease as L/a increases. The classical buckling coefficient, on the other hand, is almost constant with L/a.
2. The classical and reduced stiffness buckling coefficients asymptotically reach from bellow the horizontal line of V equals zero (G_c= ∞) . This implies that the reduced stiffness buckling strength of the axially loaded sandwich cylindrical shell is hardly improved by increasing the core shear strength at its higher values. The very same was observed even when L/a increased.
3. Both reduced stiffness and classical buckling coefficients have similar variations that all curves corresponding to different shear strengths of core merge to one line as a/h_f increases. This implies that as a/h_f increases, the contribution from the core shear strength to classical and reduced stiffness buckling strength reduces.

The reduced stiffness lower bound occurs bellow that from the FEM analysis. Further, the difference between these two indicates the effectiveness of the proposed reduced stiffness lower bound method for the axially loaded sandwich cylindrical shell. From design point of view, one of the attractive features

of reduced stiffness method is that it provides safe lower bound buckling strengths that do not depend on precise magnitude of the imperfection spectra of the shell. As a result, designers can readily apply this method without being worried about possible geometrical imperfections that might be generated during fabrication and construction of the shell. In addition, this difference indicates appropriateness of the proposed reduced stiffness method for initial sizing of the axially loaded sandwich cylindrical shell in its design process.

References

Croll, J.G.A. (1981), "Lower bound elasto-plastic buckling of cylinders", *Proc. Instn Civ. Engrs, Part 2, 71*, 235-261.

Croll, J.G.A. (1995), "Towards a rationally based elastic-plastic shell buckling methodoogy", *Thin-Walled Structures*, **23**, 67-84.

Croll, J.G.A. and Batista, R.C. (1981), "Explicit lower bounds for the buckling of axially loaded cylinders", *Int. J. Mech. Sci*., **23**(6), 331-343.

Croll, J.G.A. and Ellinas, C.P. (1983), "Reduced stiffness axial load buckling of cylinders", *Int. J. Solid Structures*, **19**(5), 461-477.

Nemeth, M.P. and Starnes (Jr.), J.H. (1998), *The NASA monographs on shell stability design recommendations, a review and suggested improvements*, Langley Research Center, Hampton, Virginia.

Ohga, M. and Umakoshi, M. (2001), "RS buckling strength of cylindrical sandwich shells under axial pressures (Japanese)", *J. of Structural Engineering*, **47A**, 27-34.

Ohga, M. and Wijenayaka, A.S. (2003), "Explicit lower bounds for imperfection sensitive buckling of axially loaded sandwich cylindrical shells", *Int. Symp. on New Perspectives of Shell and Spatial Structures*, Taipei, Taiwan, October 22-25, 156.1-8

Plantema, F.J. (1966), *Sandwich Construction: The Bending and Buckling of Sandwich Beams, Plates and Shells*, John Wiley & Sons Inc., New York, London, Sydney.

Vinson, J.R. (1999), *The Behavior of Sandwich Structures of Isotropic and Composite Materials*, Technomic Publishing Company Inc., Lancaster, PA 17604, U.S.A.

Notation

Following notations have been used in this paper.

a : mean radius of the sandwich cylinder
A_i : amplitude of the displacement function
C_{ij} : coefficients of the eigenmatrix
E_f : Young's module of the face material
E_x, E_s, E_{xs} : total membrane strains about unloaded and undeformed state
G_c : shear modulus of core material
G_f : shear modulus of face material
h : total thickness of the sandwich cylinder (h_c+2h_f)
h_c : thickness of the core
h_f : thickness of the face
k_c : classical critical buckling coefficient
k_{rs} : reduced stiffness critical buckling coefficient
L : length of the sandwich cylindrical shell
m : number of axial half waves
M_x, M_s, M_{xs} : total moment resultants

n : number of circumferential waves
q_c : classical critical buckling load
q_{rs} : reduced stiffness critical buckling load
u, v, w : incremental displacements
ν_f : Poisson's ratio of the face material
Π : total potential energy
Π_0, Π_1, Π_2 : constant, linear, quadratic components of the total potential energy
σ_x, σ_s : axial and circumferential stresses
$\tau_{xs}, \tau_{x\zeta}, \tau_{s\zeta}$: shear stress in the xs, $x\zeta$ and $s\zeta$ planes
$\varepsilon_x, \varepsilon_s$: axial and circumferential strains
$\gamma_{xs}, \gamma_{x\zeta}, \gamma_{s\zeta}$, : shear strains in the xs, $x\zeta$ and $s\zeta$ planes
α : circumferential wavelength parameter (n/a)
ρ : non-dimensional axial wavelength parameter ($m\pi / l$)
β_x, β_s : incremental rotations about s and x axes

Subscripts and Superscripts

c : belonging to classical (variational) model
fem : belonging to FEM analysis
rs : belonging to reduced stiffness model
$'$: stresses and strains that linearly dependant on displacements
$''$: stresses and strains that nonlinearly dependant on displacements

CC